

Hole-Burning Studies of the Splitting in the Ground and Excited Vibronic States of Tetracene in Helium Droplets

Matthias Hartmann,[†] Albrecht Lindinger,[‡] J. Peter Toennies,^{*} and Andrej F. Vilesov[§]

Max-Planck-Institut für Strömungsforschung, Bunsenstrasse 10, 37073 Göttingen, Germany

Received: October 2, 2000; In Final Form: April 9, 2001

The laser-induced fluorescence spectra of single tetracene (C₁₈H₁₂) and pentacene (C₂₄H₁₄) molecules embedded in liquid He_N droplets ($\bar{N} \approx 10^4$) show sharp zero phonon lines (ZPL) ($\delta\nu \leq 0.2 \text{ cm}^{-1}$), accompanied by weaker phonon wings (PW) on the blue side. The ZPL of tetracene is anomalously split into a doublet with a separation of 1.1 cm^{-1} , whereas for pentacene, the ZPL is not split. Hole-burning measurements with two pulsed dye lasers and lifetime measurements indicate that inside He droplets the ground and excited states of tetracene are each split into two levels. The splitting is attributed either to the occupation of two nearly equivalent sites by localized helium atoms or to a tunneling of one or two localized helium atoms through the barrier in the double-well potential on the surface of the tetracene molecule.

I. Introduction

Recent experiments have demonstrated that liquid helium droplets provide a uniquely gentle and very cold matrix for high-resolution molecular spectroscopy.^{1,2} In this technique single molecules are embedded inside microscopic droplets of liquid ⁴He consisting of $\bar{N} = 10^3\text{--}10^4$ atoms, produced in a cryogenic nozzle beam expansion. The special gentle nature of the matrix has been particularly impressively demonstrated in the infrared by the resolution of sharp rotational lines with a line width of about 150–300 MHz in the case of SF₆,^{3–5} OCS,^{6,7} and a number of other molecules.^{8–11} From the intensities of the rotational line structure, temperatures from 0.38 K for pure ⁴He^{3–5,7} to 0.1 K for droplets with an excess of ³He^{4,12} have been achieved. These spectra could be nicely fitted with the same Hamiltonian as for the free molecules but with quite different spectroscopic parameters^{3–5,7,11}. In particular, the moments of inertia of SF₆ and OCS are about a factor of 3 larger than those of the free molecules^{3,6,7}. This has been attributed to the effect of 8 and 6 He atoms, respectively, which participate in the overall end-over-end rotations of the molecule. Both theory¹³ and other spectroscopic experiments¹⁴ indicate that the droplets are superfluid and the ability for molecules to rotate freely appears to be a microscopic manifestation of superfluidity.⁶ These extensive spectroscopic experiments and Monte Carlo and density functional calculations^{2,15,16} all indicate that closed-shell molecules are strongly “heliophilic” and as a consequence reside near the center of the droplets. Alkali and alkaline earth metal atoms and their small clusters have been shown to be “heliophobic”¹⁶ and from spectroscopic studies^{17,18} it is known that they are attached to the surface of helium droplets.

The first measurements of spectra in the visible region were obtained for the S₁ ← S₀ transition in glyoxal.¹⁴ The spectrum consisted of a sharp ($\delta\nu \leq 0.1 \text{ cm}^{-1}$) zero phonon line (ZPL) accompanied by a phonon wing (PW) on the blue side. The ZPL,

which is well-known in matrix isolation spectroscopy¹⁹ corresponds to a pure electronic transition, whereas the PW originates from the simultaneous excitation of collective excitations inside the droplet. The shape of the PW could be nicely simulated using the *sharp* bulk helium dispersion curve for elementary excitations, which is a characteristic feature of the superfluid state.^{20,21} Although the elementary excitations in superfluid helium consist of phonon, maxon, and roton features,^{20,21} in this article they will be referred to collectively as “phonons”.

In the present investigation the spectroscopic studies have been extended to the large symmetric planar organic molecules tetracene (C₁₈H₁₂) and pentacene (C₂₄H₁₄). The spectroscopy of these molecules is well-known from matrix isolation^{22,23} as well as from the seeded nozzle beam experiments^{24–30}. The free molecules have the advantages of having large quantum yields for fluorescence ($Y > 0.1$)³¹ and narrow homogeneous line widths ($\Delta\nu = 10\text{--}30 \text{ MHz}$),^{22,23} important for high-resolution studies. Previously, we have also reported on the vibronic spectra of tryptophan,³² tyrosine,³² C₆₀,³³ and BaO,³⁴ and additional results are available for naphthalene,³⁵ several indoles, tryptamine and *N*-acetyltryptophan³⁶ as well as porphyrin and phthalocyanine.³⁷ The vibronic spectra of tetracene–Ar van der Waals complexes formed inside He droplets have already been described in an earlier publication.³⁸ The vibronic spectra of all these large molecules in He droplets exhibit sharp spectral features even though, in contrast to glyoxal, He atoms are expected to be more strongly bound to large organic molecules. These experiments nicely confirm the advantages of the ultralow temperatures and the gentle nature of superfluid helium droplets that make them an ideal spectroscopic matrix also in the visible.

In contrast to pentacene and several of the other molecules mentioned above, the ZPL of tetracene reveals a distinct splitting of 1.1 cm^{-1} .^{38,39} To investigate the origin of this splitting, the results of hole-burning measurements with two pulsed dye lasers delayed by $\Delta t > 100 \text{ ns}$ are reported here. The measurements reveal the existence of two closely spaced levels in the ground S₀ state. In addition, time-resolved measurements of the induced fluorescence intensity after pulsed excitation of each of the two lines reveal different lifetimes, providing evidence that the electronically excited S₁ state is also split into two levels. These

* Corresponding author. E-mail: jtoenni@gwdg.de.

[†] Present address: BMW AG, 80788 Munich, Germany.

[‡] Present address: Dept. of Chemistry, University of California in Berkeley, Berkeley CA 94720-1460.

[§] Present address: Department of Chemistry, University of Southern California, Los Angeles CA 90089-1062.

results are interpreted by assuming two configurations or states of the surrounding helium, designated α and β , each with a slightly different matrix shift that manifests itself as a splitting into two lines. Three simple models are presented that explain the splitting either in terms of the occupation of two nearly equivalent sites by localized helium atoms or by a tunneling of one or two localized He atoms, which are tightly bound to equivalent sites at the surface in the central region of the tetracene molecule. The third mechanism combines features of both of the above models. These models all assume the presence of localized He atoms on the surface of the impurity molecules and thereby they complement earlier evidence for the attachment of a number of He atoms from the superfluid environment that participate in the rotations of the impurity molecule.^{3,5–7} This idea has now received support from recent path integral Monte Carlo calculations.⁴⁰

The present article begins with a brief description of the experimental techniques in section II. Then the results on the LIF spectroscopy of the tetracene and pentacene in He droplets are reported in section III. In section IV the simple models involving localized He atoms are described. Section V gives a summary of the obtained results.

II. Experimental Aspects

The apparatus is very similar to the one described in refs 1, 5, and 7. Droplets of ⁴He are formed by expanding 99.9999% pure ⁴He through a 5 μ m diameter orifice from a source at a stagnation pressure of $P_0 = 20$ bar and temperatures between $T_0 = 10$ and 15 K.⁴¹ The corresponding average droplet sizes have been characterized by several different experimental techniques^{1,5,42} and lie between about $\bar{N} = 2 \times 10^4$ and $\bar{N} = 10^3$ atoms, respectively. At a distance of 10 cm downstream from the source, the droplets pass through a 1 cm long scattering cell containing the powder of the corresponding substance. Prior to the experiments the cell was heated in situ to about 100 °C for about 3 h to remove adsorbed water. The temperature of the cell was maintained at 130 C for tetracene and 180 C for pentacene to provide a vapor pressure for each gas of about 10^{-3} mbar,^{43,44} needed to capture on average a single molecule per droplet. Commercially available tetracene and pentacene⁴⁵ were used without further purification. Because of leakage through the large entrance and exit holes (5 mm diameter) of the scattering cell the actual effective pressure is estimated to be 10^{-4} mbar,^{35,46} which is less than the equilibrium vapor pressure. To prepare tetracene complexes with a single Ar atom argon gas was admitted at a pressure of 5×10^{-7} mbar to the main a vacuum chamber as described in ref 38. The capture of these molecules by the droplets was detected by a quadrupole mass spectrometer located at 100 cm from the source.⁴⁷ The mass spectra were dominated by peaks at the mass of the unfragmented molecule or with loss of a single proton demonstrating a low fragmentation of the ionized molecules and high purity of the embedded molecules.

In the present experiments photon absorption was detected via laser-induced fluorescence (LIF), which was more efficient than the commonly used depletion method¹. A pulsed (pulse length 20 ns) excimer pumped dye laser⁴⁸ (repetition rate 71 Hz) was used with various dyes chosen for excitation in the region of the band origin of the $S_1 \leftarrow S_0$ transitions. The laser beam was unfocused, had a diameter of about 2 mm, and crossed the droplet beam at right angles 6 cm downstream from the scattering chamber. The line width of the laser was typically 0.5 cm^{-1} and was narrowed to about 0.1 cm^{-1} with an intracavity Etalon for some experiments. The wavelength was

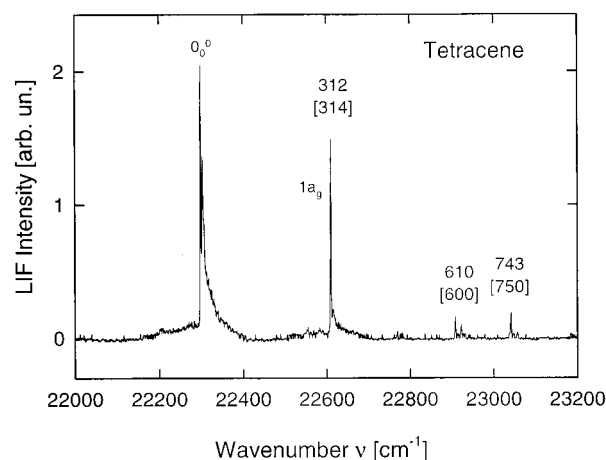


Figure 1. LIF spectrum of single tetracene molecules embedded in He droplets. The ⁴He source conditions were $P_0 = 20$ bar and $T_0 = 11$ K, and the mean droplet size is estimated to be $\bar{N} = 1.5 \times 10^4$. The laser output energy was $E_{\text{las}} = 0.5$ mJ/pulse. The transition and the frequencies relative to the 0_0^0 origin are listed, the numbers in brackets are the corresponding frequencies of the free molecule.²⁴

calibrated against the spectrum of a optogalvanic Al–Ne lamp. This procedure is expected to give an absolute precision of $\pm 1 \text{ cm}^{-1}$ in the quoted vacuum wavenumbers.

The laser-induced fluorescence was collected by a lens system ($f/2$) at right angles to the droplet and dye laser beams and the photons were detected by a photomultiplier⁴⁹ connected to a boxcar integrator⁵⁰ having a gate of typically 50 ns triggered directly without delay by the laser pulse. To reduce the laser stray light, color filters were inserted in front of the photomultiplier having a cutoff at typically 25 nm on the red side of the excitation line. Time-resolved LIF were measured using an ultrafast (5 ns/channel) time-of-flight module⁵¹ in a single photon counting mode.

A second similar pulsed dye laser that overlapped the beam of the first laser was used for the hole-burning experiments. The time between the two laser pulses could be varied between $\Delta t = 100$ and 1000 ns. The delay between the two pulses fluctuated to within 50 ns, which is attributed to a jitter in the switching of the thyatron of the excimer lasers.

III. Results

A. LIF Lifetime Measurements. Figure 1 shows an overview LIF excitation spectrum of single tetracene molecules in helium droplets in the range of 22 000–23 200 cm^{-1} . The four sharp features, which are quite similar to those of the free molecule spectrum^{24,30} except that they exhibit exponential tails toward the blue, are due to vibronic transitions between the ground state S_0 and the first excited singlet state S_1 of a tetracene. The 0_0^0 band corresponds to an electronic transition involving the lowest vibrational states of the S_0 and S_1 states. Transitions at higher frequencies correspond to the excitation of totally symmetric vibrations in the S_1 state. Table 1 compares the frequencies of these vibrations with those in the free molecules. Surprisingly, there is only a small shift of about 1–2 cm^{-1} .

Figure 2 shows the spectra on an enlarged frequency scale in the vicinity of the 0_0^0 band as measured with two different laser energies. The sharp lines α and β are assigned to ZPL transitions, whereas the broader structure on the blue side is a PW. The ZPL of the 0_0^0 band is split by 1.1 cm^{-1} , which is not seen in the free molecules. The α -line of the 0_0^0 transition at $\nu = 22\,293.4 \pm 0.5 \text{ cm}^{-1}$ is red shifted by $104.0 \pm 0.5 \text{ cm}^{-1}$ with respect to the 0_0^0 line in the free molecule.³⁰ The intensity

TABLE 1: Positions of 0_0^0 Bands (in a Vacuum) and Vibrational Frequencies in the S_1 State (cm^{-1}) for Free Molecules and for Molecules in He Droplets

transition	free mol	mol in He drop.	line shift ^b
Tetracene			
0_0^0	22 397.4 ^c	22 293.4 \pm 0.5 ^a	-104.0 \pm 0.5
1	310 ^d	312 ^a	+2
2	609 ^d	610 ^a	+1
3	741 ^d	743 ^a	+2
Pentacene			
0_0^0	18648.996 ^d	18545.0 \pm 0.5	-104.0 \pm 0.5
1	77 ^e	85	+12
2	202 ^e	207	+5
3	263 ^e	256	-7
4	345 ^e	340	-5

^a For tetracene the frequency of the α lines is quoted. ^b For vibronic transition the vibrational frequency shift is given. ^c Reference 30. ^d Reference 55. ^e Reference 25.

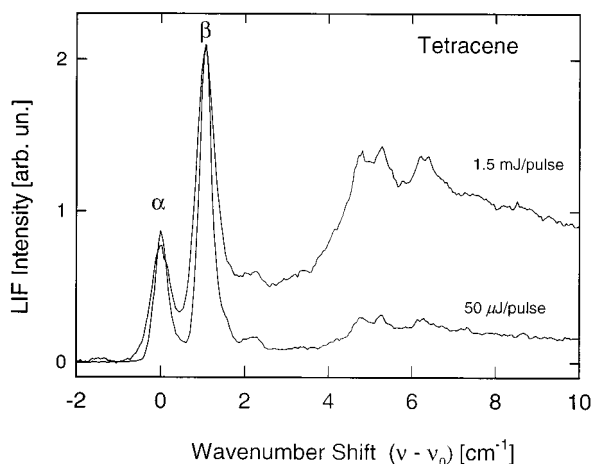


Figure 2. LIF spectra of single tetracene molecules in the region of the 0_0^0 band as measured for different laser output energies. $E_{\text{las}} = 1.5$ mJ/pulse; and $E_{\text{las}} = 0.05$ mJ/pulse. The ^4He source conditions were $P_0 = 20$ bar, $T_0 = 11$ K, and the mean droplet is estimated to be $\bar{N} = 1.5 \times 10^4$. Zero energy corresponds to the maximum of the ZPL at $22\,293.4 \pm 0.5$ cm^{-1} . The spectra were recorded with a time constant of 3 s.

of the PW relative to that of the ZPL increases with laser power. This behavior was also observed in our previous work with glyoxal¹⁴ and was attributed to laser power saturation of the strong ZPL transitions which in the gas phase have an oscillator strength $f \approx 0.1$.²⁴ Moreover, the ratio of the LIF intensities for the β and α lines was also found to be dependent on the laser pulse energy increasing gradually from $I_\beta/I_\alpha = 1.5$ for low laser power of $E_{\text{las}} = 10$ $\mu\text{J}/\text{pulse}$ to $I_\beta/I_\alpha = 2.9$ for $E_{\text{las}} = 5$ mJ/pulse. With depletion detection the intensity ratio was $I_\beta/I_\alpha = 1.4$ and remained constant for laser pulse energies in the range of 0.1 to 10 mJ/pulse.

Parts a and b of Figures 3 show a comparison of the ZPL Etalon spectra in the vicinity of the band origin for two different mean droplet sizes. The decrease in line width with increasing droplet size, which was observed previously for SF_6 ,⁵ is presumably due to residual inhomogeneous broadening resulting from the large spread in the droplet sizes.⁴² Because of the finite size of the droplet, the molecule, which is assumed to be at the center of the droplet, “feels” to some extent the surface. The spectral shift of the band origin in a droplet relative to that for free molecule $\Delta\nu(N)$ is therefore somewhat smaller than in an infinite medium $\Delta\nu(\infty)$. According to the excluded volume theory⁵² the quantity $\Delta\nu(\infty) - \Delta\nu(N)$ scales as $1/N$, where N is

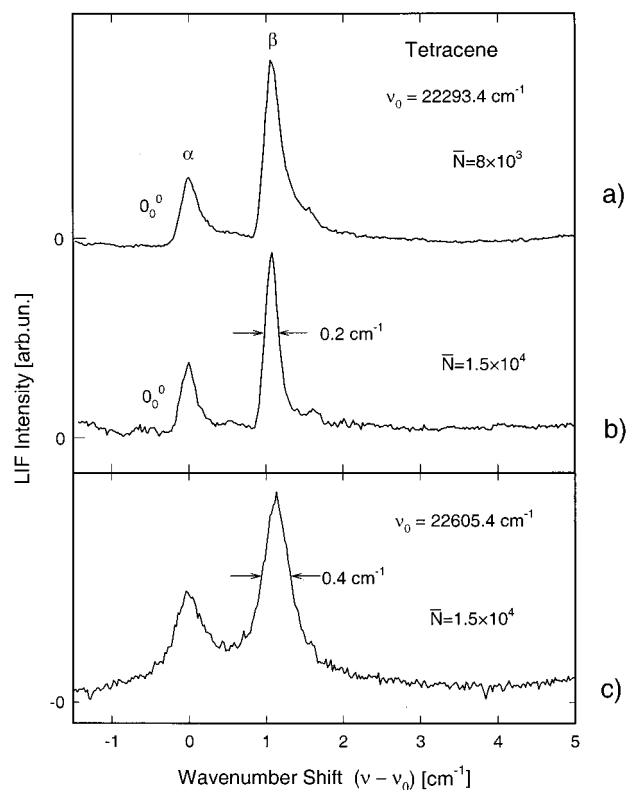


Figure 3. LIF Etalon scans of single tetracene molecules in He droplets for the 0_0^0 transition ZPL for two different droplet sizes (a) and (b) and for the $\nu = 312$ cm^{-1} vibronic transition (c). The laser output energy was $E_{\text{las}} = 5$ μJ for (a) and (b) and $E_{\text{las}} = 25$ μJ for (c).

the size of the droplet. For the known log-normal droplet size distribution⁴² ($\Delta N \approx 0.8\bar{N}$) the inhomogeneous line width can be easily shown to be proportional to N^{-1} . This explains the reduction in line width seen in Figure 3b compared to Figure 3a. Since for the large droplets ($\bar{N} \approx 1.5 \times 10^4$) the line width is comparable to the line width of the dye laser (0.1 cm^{-1}) a further reduction in line width could not be measured. It is interesting to note that the infrared rovibrational transitions in SF_6 approached their asymptotic width already for $\bar{N} \approx 3 \times 10^3$. Thus, it appears that the vibronic transitions are more sensitive to size effects.

The scans over the vibronic band at 312 cm^{-1} (see Figure 3c) reveal similar structure with a somewhat larger splitting of 1.2 cm^{-1} . Etalon scans give a line width of about 0.4 cm^{-1} , considerably broader than that for the 0_0^0 band. The fact that vibronic bands are broader than the 0_0^0 band origin is well-known from isolation spectroscopy in solids and is attributed to vibrational relaxation within the S_1 state.²²

Figure 4 shows the result of the time-resolved LIF measurement for the lines α and β of the 0_0^0 , respectively. Different lifetimes of $\tau_\alpha = 23 \pm 3$ ns and $\tau_\beta = 35 \pm 3$ ns are found for the lines α and β , respectively. This can only be explained if the upper states of the transitions α and β are different. The lifetime of the free tetracene molecule in the S_1 state in the 0_0^0 band has been reported to be 20 ± 2 ns²⁴ in close agreement with the lifetime of the α -line.

B. Hole-Burning Experiments. To provide further insight into the origin of the splitting of the ZPL, hole-burning experiments with two lasers were performed. In these experiments the frequency of the first laser was adjusted on the maximum absorption of one of the two lines. The second laser, triggered after delays Δt between 100 and 1000 ns, scanned the spectrum in the range of the two ZPL lines. A combination

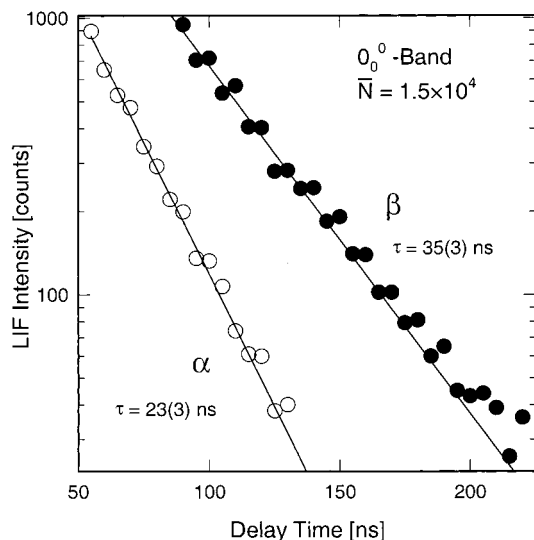


Figure 4. Time-resolved LIF intensity is plotted as a function of time after excitation of either the α or β lines of the ZPL of tetracene molecules. The mean droplet size was $\bar{N} = 1.5 \times 10^4$. The time resolution was 5 ns per channel.

of a cutoff filter (<475 nm) and a neutral filter was used in order to avoid any saturation of the photomultiplier during the hole-burning pulse. The ratios of the LIF intensities integrated over the first and the second line, I_α and I_β , were measured as a function of the time delay between the two laser pulses for different pulse energies of the first laser pulse. Figure 5a shows the results of these measurements when the hole was burned on the frequency of the β line for the three indicated pulse energies of the burning laser. The probing laser was operated at 0.01 mJ per pulse. It is seen that the ratio of I_β/I_α increases significantly for $\Delta t < 200$ ns. At larger delay times this ratio levels off to a value between 1.5 and 2.3 depending on the laser power. These values are considerably lower than the value $I_\beta/I_\alpha = 2.9 \pm 0.2$ measured without hole burning and strongly suggest that the ground state also consists of two split energy levels.

The rise of the ratio I_β/I_α at short delay times can be explained by noting that after the initial strong depletion of the β line via the pumping of the $S_1 \leftarrow S_0$ transition the population may return back to the S_0 state via fluorescence or internal conversion into an excited vibrational state followed by vibrational relaxation. Thus, the behavior of I_β/I_α at short delays provides information on the rates of these processes. The S_1 population prepared by the initial laser pulse may also undergo an intersystem crossing within the long-lived triplet state and as a consequence a persistent hole may be created in the population of the pumped ground state. The magnitude of the hole will be independent of the delay time between the laser pulses if it is shorter than the characteristic relaxation time of the triplet state and the time-of-flight of the droplets through the laser beam, which is about 5 μ s in the present experiments. If the ground-state levels are distinct then the ratio I_β/I_α is expected to behave in the opposite way after burning on the frequency of the α line, as indeed is found as shown in Figure 5b. Therefore, we conclude that the two ZPLs in the spectrum of a tetracene in liquid helium have different ground states. Unfortunately, from the spectra there is no way to estimate the spacing of the two ground-state levels. By assuming that these levels are in equilibrium with the helium bath, a rough estimate can be made on the basis of the Boltzmann factors at the low temperature of 0.38 K (0.26 cm^{-1}) of the droplets. Accordingly, only if the splitting is of the order of the ambient temperature will both levels be equally populated.

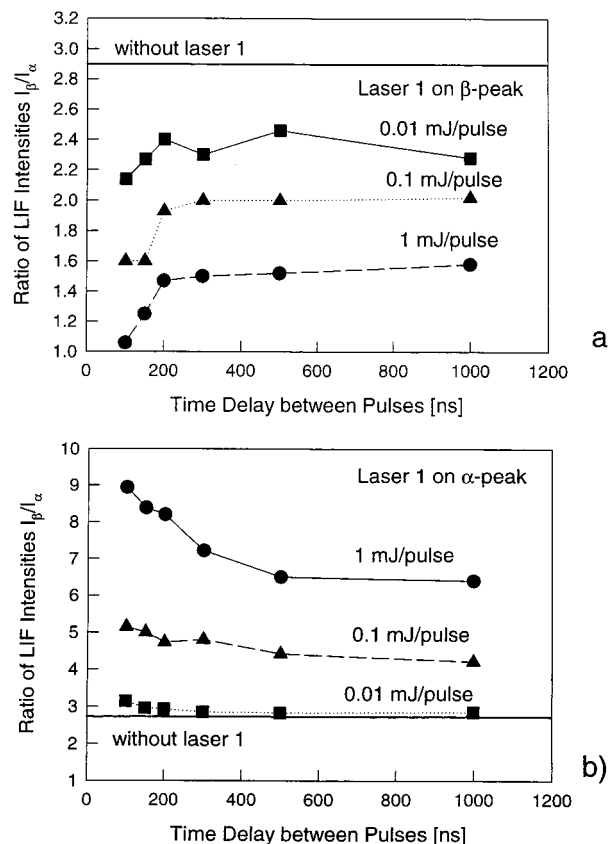


Figure 5. Results of the hole-burning experiments showing the intensity ratio I_β/I_α of the α and β components of the ZPL of single tetracene molecules in He droplets ($\bar{N} = 1.5 \times 10^4$) as a function of the time delay between the two laser pulses for the indicated pulse energies of the hole-burning laser. The intensity ratios measured without the hole-burning laser are shown by the straight horizontal lines. In (a) the hole was burned on the β line, and in (b) on the α line. $I_\beta/I_\alpha = 2.9 \pm 0.2$ was measured without the first laser. The laser output energy of the scanning laser was $E_{\text{las}} = 0.01$ mJ/pulse.

Thus, the splitting in the ground state will be less than about 0.26 cm^{-1} and in the excited state about 1 cm^{-1} . If these levels are metastable, then the above considerations are no longer valid and a much larger splitting of the levels is conceivable.

Another interesting observation is the increase of the absolute intensity of the α -peak intensity I_α after pumping the β -line. This effect is most clearly observed for the experiments with the largest energy of the hole-burning pulse. It amounts to 25% of the I_α intensity and is independent of the delay time in the range 200–1000 ns. This can be explained by an interconversion between the two ground-state spectral isomers after excitation of the S_1 state. This observation provides evidence that the two ground states leading to the observed ZPLs are a feature of one and the same tetracene molecule. Figure 6 shows diagram with the split energy levels of tetracene in He droplets and possible relaxation pathways to be discussed in a following article.⁵³

C. Possible Origins of the Splitting in Tetracene. The above experiments have established that the splitting is an inherent property of the ground and excited electronic states of a single molecule in liquid helium but do not provide any evidence for the mechanism leading to the splitting. One obvious possibility is that it is due to partially resolved rotational structure. The rotational constants of a free tetracene molecule have been measured to be $A = 1630$ MHz, $B = 213$ MHz, $C = 189$ MHz²⁸ indicating a nearly symmetric prolate top molecule. From measurements made for SF_6 ^{3–5} and OCS ^{6,7} the rotational constants in liquid helium are expected to be about 3 times

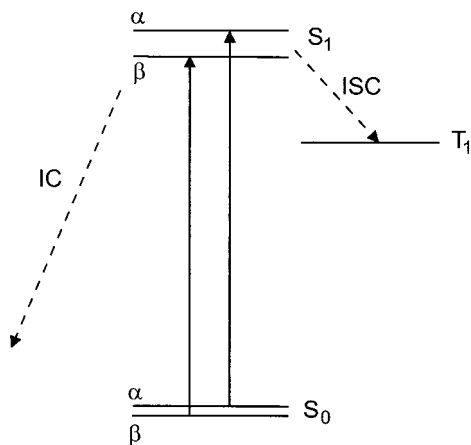


Figure 6. Schematic diagram showing the α - β level splitting of the ground S_0 and excited S_1 electronic states of tetracene in ^4He droplets. The possible relaxation pathways via intersystem crossing (ISC) to the dark T_1 state or via internal conversion (IC) back to the ground state are indicated schematically.

smaller than for the free molecule. Assuming the same reduction for tetracene the half-width of the entire rotational envelope of the 0_0^0 band for $T = 0.38$ K can be estimated to be 0.2 cm^{-1} , which is much less than the splitting. The hole-burning spectra have also been measured previously in ref 30 for the free molecule in seeded beams. The observed hole spectra of the 0_0^0 band closely resembles the excitation spectra having partially resolved P and R branches. Both of these observations strongly suggest that the observed splitting cannot be due to unresolved rotational structure. Finally, the possibility that the splitting is from hot bands can be ruled out by the low temperature of the droplet.

Another possible origin of the splitting might be an isotope shift. Because of the 1% natural abundance of ^{13}C atoms, about 19% of the tetracene molecules are expected to have one or more ^{13}C atoms.²⁸ To check for this, the ion signals due to the different isotopes were separated in the quadrupole mass spectrometer and the depletion spectra recorded. The spectrum measured on the mass of $^{12}\text{C}_{18}\text{H}_{12}^+$ (dominant ion peak) revealed the same split structure as the LIF spectrum in Figure 2,³⁹ indicating that a tetracene isotopomer is not responsible for the observed splitting.

To investigate further the origin of the observed sharp spectra, a tetracene molecule and an Ar atom were picked up sequentially to allow a tetracene-argon van der Waals complex to be formed inside the droplet.³⁸ The Ar atom is expected to reside over one of the two central rings of the tetracene where the potential energy of the van der Waals complex is predicted to have its two deepest van der Waals wells, with equal well depth.²⁷ Figure 7 shows the spectrum of the tetracene-argon complex in the vicinity of the band origin which is shifted to the red by 37 cm^{-1} relative to the spectrum of the single tetracene molecule, Figure 2. The spectrum shows clearly that the splitting of the ZPL is quenched upon the addition of the Ar atom. Thus, the observed sharp spectra are very sensitive to the symmetry of the tetracene molecular environment.

In an attempt to show that the splitting is a feature of the He droplets, the LIF spectra of tetracene were also measured with H_2 clusters. For this purpose, H_2 clusters with about $\bar{N} = 5 \times 10^3$ molecules were produced by expanding pure H_2 gas at $T_0 = 56$ K and $P_0 = 40$ bar and doped with tetracene molecules in the same way as described for He droplets. There is now some evidence that H_2 clusters produced under these conditions are fluidlike and probably are not solid.⁵⁴ The LIF spectrum of

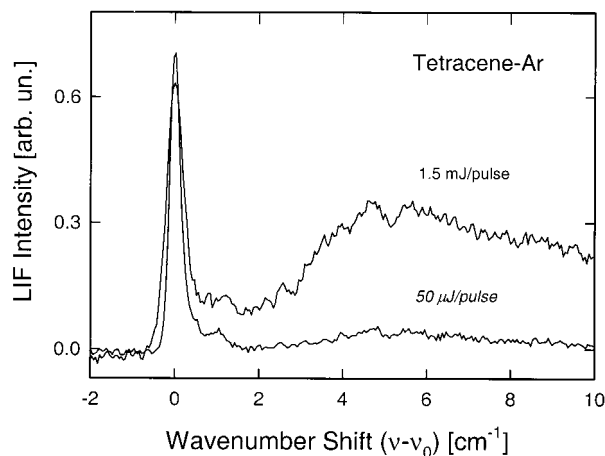


Figure 7. LIF spectra in the region of the ZPL tetracene Ar van der Waals complexes formed inside ^4He droplets ($\bar{N} = 1.5 \times 10^4$) measured for different laser output energies. $E_{\text{las}} = 1.5$ mJ/pulse and $E_{\text{las}} = 50$ μJ /pulse. Zero energy corresponds to the maximum of the ZPL at $22\,256.3 \pm 0.5$ cm^{-1} .

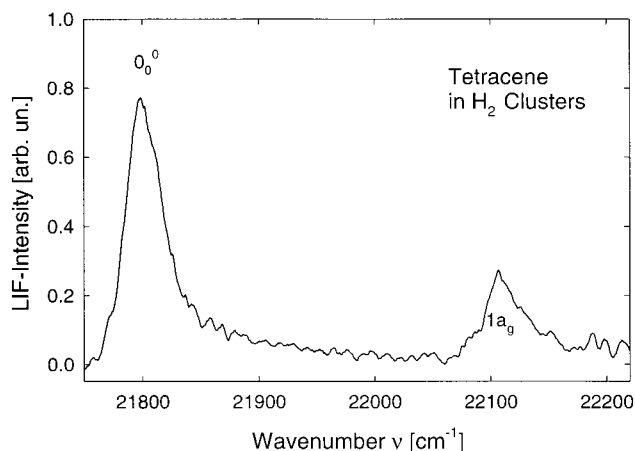


Figure 8. LIF spectrum of single tetracene molecules embedded in normal- H_2 ($n\text{H}_2$) clusters. The $n\text{H}_2$ source conditions were $P_0 = 40$ bar, $T_0 = 56$ K, and the mean droplet size was estimated to be $N = 5 \times 10^3$.⁵³

tetracene in H_2 clusters shown in Figure 8 is red shifted by about 570 cm^{-1} with respect to the gas phase. Since both the 0_0^0 and the $1a_g$ (312 cm^{-1}) bands appear as broad ($\Delta\nu \approx 40$ cm^{-1}) and structureless features with tails extending toward the blue, it was, unfortunately, not possible to identify any ZPL splitting nor was it possible to observe the phonon wing. The tails are probably due to inhomogeneous broadening in the H_2 clusters. The much broader spectrum found for H_2 clusters does, however, nicely confirm that the sharp vibronic spectra are a special property of He droplets.

To explore the possible influence of the molecular symmetry, the pentacene molecule was also investigated. Figure 9 shows an overview spectrum of pentacene in He droplet. The 0_0^0 band origin is at $\nu_0 = 18\,545.0 \pm 0.5$ cm^{-1} relative to $\nu = 18\,648.996$ cm^{-1} for the free molecule,⁵⁵ corresponding to a red shift of $\Delta\nu = 104.0$ cm^{-1} , and is similarly sharp as in tetracene. The shift is equal to the value of 104.0 ± 0.5 cm^{-1} found for tetracene. The vibronic bands at $\Delta\nu = 85$, 207 , and 340 cm^{-1} are considerably broadened ($\delta\nu = 7$ cm^{-1}) with respect to the 0_0^0 band and the band at $\nu = 263$ cm^{-1} . They are assigned to the large amplitude butterfly vibrations of the pentacene molecule and their overtones since they are similar to the corresponding free molecule frequencies at $\Delta\nu = 77$, 202 , and

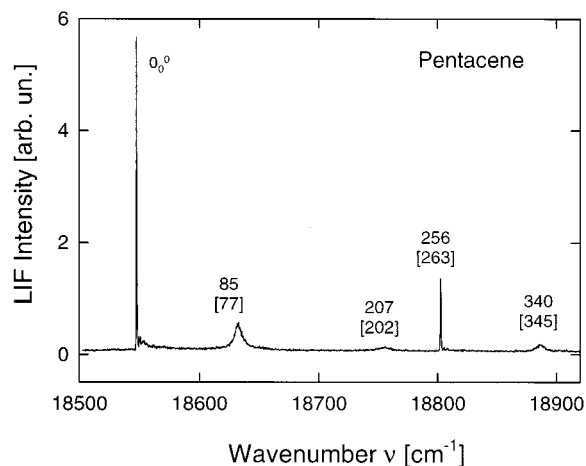


Figure 9. LIF spectrum of single pentacene molecules embedded in He droplets ($\bar{N} = 1.5 \times 10^4$). The laser output energy was $E_{\text{las}} = 0.03$ mJ/pulse. The transition and frequencies relative to be 0_0^0 origin are listed, the numbers in brackets are the corresponding frequencies of the free molecule.²⁵

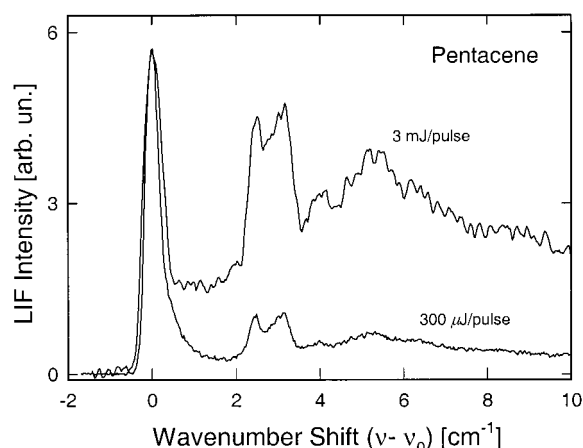


Figure 10. LIF spectrum of single pentacene molecule in the region of the ZPL in ^4He droplets ($\bar{N} = 1.5 \times 10^4$) measured for different laser output energies of $E_{\text{las}} = 3$ mJ/pulse and $E_{\text{las}} = 300 \mu\text{J/pulse}$.

345 cm^{-1} , with respect to the free molecule origin ν_0 .²⁵ The considerable broadening of this vibrational mode suggests that these butterfly motions, although their frequencies are nearly the same as in the gas phase, are more strongly perturbed by the helium than the other modes. In support of this interpretation it is noted that these lines are not found in solid matrixes.²⁵ The narrow line at 263 cm^{-1} has so far not been assigned.²⁵

Figure 10 shows a high-resolution spectrum in the region of the 0_0^0 band of pentacene at two different laser pulse energies. The ZPL appears as a single sharp peak ($\delta\nu \sim 0.5 \text{ cm}^{-1}$) without any splitting. This is interpreted as indicating that the structural symmetry of the molecule has an effect on the appearance of the splitting. It is interesting to see new features at 2.3 and 3.2 cm^{-1} in the phonon wing not found in tetracene, in addition to the maximum at about 5.3 cm^{-1} seen in tetracene. Similar inelastic features have also been found for porphyrin and phthalocyanine and will be discussed in a forthcoming paper.³⁷

IV. Discussion

The experimental results discussed above, especially the tetracene–Ar and the pentacene spectra indicate that the presence of *two* adjacent inequivalent sites of strong binding at the surface of the molecule is an essential requirement for the

splitting to occur. From extensive Monte Carlo and density functional calculation it is now well established that as a result of the strong van der Waals potential of closed-shell molecules these are invariably heliophilic^{2,15,16}. Since the He atom–molecule potential is considerably stronger than the weak He–He interaction ($\epsilon \sim 11 \text{ K}$) there is a considerable increase of the density of the He atoms in the immediate vicinity of the molecule, and at least for atomic and nearly spherical foreign molecule impurities, well-defined solvation shells are created around the particles. The available calculations^{2,15,16} show that the density increase at the maximum, n_{max} , corresponding to the first shell, correlates with the well depth ϵ as $n_{\text{max}} (\text{\AA}^{-3}) = 2.1 \times 10^{-3}\epsilon[\text{K}]$.⁵⁶ This increase of density is large and a factor 4 greater than in the bulk liquid and corresponds to that of solid helium. A comparison with the bulk is, however, not justified since most of the effect is of a local nature and appears to be due to an increased radial ordering⁵⁷ so that the helium atoms in the first shell are probably highly mobile within the surface shell.⁵⁸ Moreover, path integral Monte Carlo calculations reveal that a sizable fraction of the first solvation shell He atoms participate in permutation exchanges with atoms further away from the molecule. In anisotropic molecules such as SF_6 and OCS there is now extensive experimental^{3,7} and theoretical evidence^{58,59} that the first solvation shell He atom density is unevenly distributed over the surface of the molecule and is concentrated in regions where the potential well depth is deepest.

To further explore the effect of the anisotropic He–tetracene van der Waals potential, a model potential was generated using a summation of two-body semiempirical potentials which had been used previously to simulate the corresponding free complex spectra²⁷ for the heavier rare gases. The following Lennard-Jones (12–6) potential parameters were used. He–C atom: $\epsilon = 1.40 \text{ meV}$ (11.291 cm^{-1} , 16.2 K) and $r_0 = 2.74 \text{ \AA}$. He–H atom: $\epsilon = 0.517 \text{ meV}$ (4.169 cm^{-1} , 6.0 K) and $r_0 = 3.21 \text{ \AA}$, where ϵ is the well depth and r_0 is the distance at which the potential passes through zero.

Figure 11a shows the potential energy contours calculated for a fixed distance of $Z = 2.7 \text{ \AA}$ of the He atom above the plane of the tetracene molecule. The four minima at $Y = 0 \text{ \AA}$ are located above the centers of the four “benzene” rings of the molecule. Since the inner two wells are shielded from the edges their depths are somewhat greater. This is seen more clearly in Figure 11b, where the potential energy surface is plotted in the X, Z plane passing through the center of symmetry of the molecule ($Y = 0$). Other calculations for similar planar organic molecules²⁷ confirm that these central minima have the deepest wells of the entire potential surface. From our empirical rule for n_{max} for spherical systems the density increase in these minima is crudely estimated to be a factor 15 greater than the bulk liquid density. This large density increase is consistent with neutron scattering experiments on graphite inside bulk liquid helium⁶⁰ and related theoretical phase diagrams.⁶¹ Depending on the strength of the van der Waals potential either a liquidlike layer, one or two solidlike layers are expected.⁶¹ On the graphite surface two solid like layers are expected on the basis of this correlation.

These observations suggest that these double-well positions are occupied by one or possibly two localized He atoms. There are many spectroscopic studies of free van der Waals clusters with one or more attached He atoms to molecules with ring structures such as benzene,⁶² aniline,^{63,64} tetrazine,⁶⁵ indole,⁶⁶ stilbene,⁶⁷ and anthracene.⁶⁴

Before proceeding further, it is necessary to point out that the two central well positions on tetracene are spaced apart by

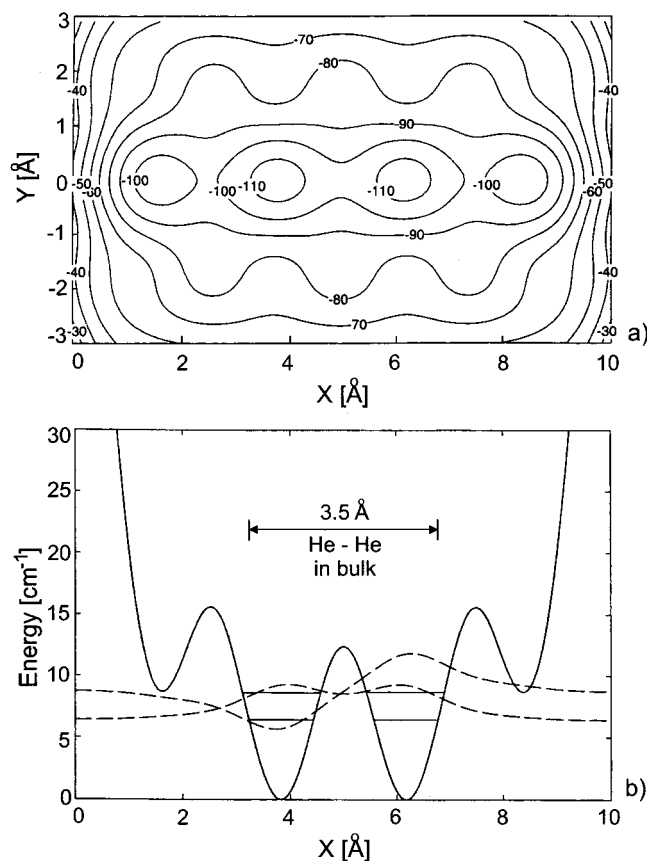


Figure 11. Two sections of the van der Waals potential surface between a single He atom and a free tetracene molecule. In (a) the equipotential lines are shown in the plane of the tetracene surface for a fixed distance of $Z = 2.7$ Å of the He atom above the molecule. In (b) the potential energy is shown along the X -direction at $Y = 0$ and $Z = 2.7$ Å. The energy levels and corresponding wave functions (dashed curves) calculated for one-dimensional motions are also indicated.

only 2.5 Å, which is much smaller than the average distance of about 3.5 Å between He atoms in the bulk liquid.⁶⁸ This suggests that it is energetically more favorable for He atoms to occupy either one or the other of the well positions. With these boundary conditions the potential surface (Figure 11) suggests three scenarios shown schematically in Figure 12. In one of these (model I) two He atoms occupy one of the well sites at the top face of the molecule and one well site at the bottom. The α - β splitting is due to small differences in the energy that arise when the two atoms are directly opposite each other or are diagonally opposite each other. The line shifts for addition of one He atom to the cyclic molecules studied so far vary [-1.1 cm⁻¹ (aniline), -1.38 cm⁻¹ (tetrazine), $+2.4$ cm⁻¹ (indole), -6.5 cm⁻¹ (stilbene)] and are of about the correct magnitude. The addition of a second He atom to the opposite side leads invariably to about twice this shift.^{69,70} Such states could so far not be resolved for the free He-tetracene complexes but have been assigned to the spectra of complexes with the heavier rare gases.^{26,28} In our earlier study of tetracene-Ar_{*N*} clusters there were several unidentified lines in the region of the spectrum that could correspond to these isomers, however.³⁸

Another possible scenario (model II) is one in which one localized He atom is able to tunnel back and forth between the two wells without being appreciably disturbed by the other surrounding He atoms. To obtain at least a simple estimate of the expected splitting, the Schrödinger equation for the tunneling of a single atom in one dimension corresponding to the potential

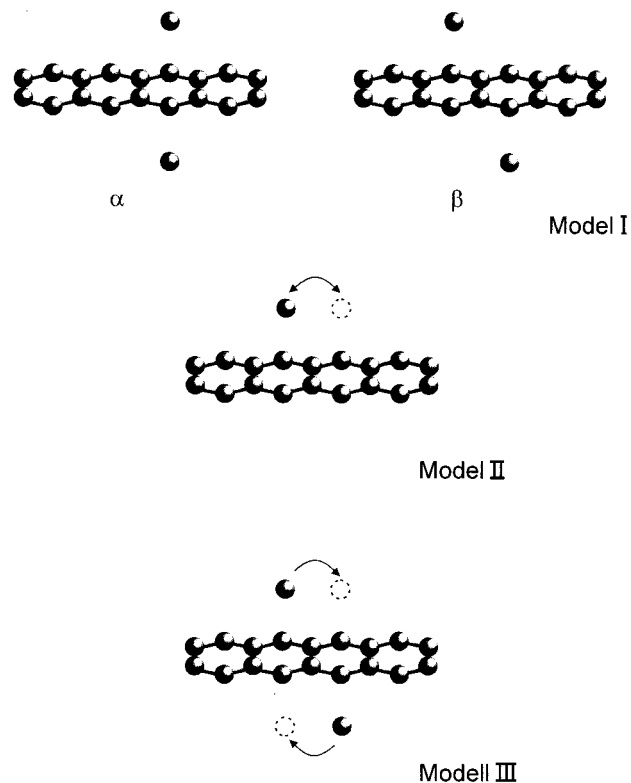


Figure 12. Schematic diagram of the three different models discussed in the text to explain the α - β splitting of the ZPL of tetracene in ⁴He droplets.

in Figure 11b was solved.⁷¹ The wave function and splitting are also shown in Figure 11b. The predicted splitting of the ground state is $\Delta E = 2.3$ cm⁻¹ in order-of-magnitude agreement with the estimated splitting of the ground state of ≤ 0.26 cm⁻¹ based on the assumption of thermal equilibrium. In view of the one-dimensional nature of the model and the neglect of the interactions with the other bath atoms, the one-dimensional model is expected to only provide a very rough upper limit.⁷²

The occurrence of tunneling inside bulk solid and liquid helium is favored by the large root-mean-squared amplitudes of vibrations, which in solid bcc ⁴He can approach 30% of the nearest neighbor distance.⁷³ This enables two ⁴He atoms in adjacent sites to encounter one another far from their equilibrium sites and tunnel past each other and exchange lattice sites. In the case of two ⁴He atoms, however, only symmetric wave functions are allowed in view of the Boson nature of the particles. In solid ³He NMR, experiments indicate that the energy associated with the exchange process is, however, only about 1 mK ($\approx 7 \times 10^{-4}$ cm⁻¹).⁷⁴ Estimates in liquid ⁴He indicate even much smaller exchange energies of only about 3 μ K.⁷⁵ Similar tunneling phenomena also occur among the hydride protons in metal dihydrides and trihydrides, where the exchange energy amounts to at most about 10³ Hz (5×10^{-8} K).⁷⁶

One shortcoming of this model is that it is not clear as to whether one atom is hopping between adjacent sites or if, as in the calculations have been carried out for bulk ³He and ⁴He as discussed above, two or more atoms are involved. Another flaw of the model is that it is not clear how to account for the possibility that tunneling should occur on both sides of the molecule and what effect this would have. Moreover the suppression of the splitting by the addition of one Ar atom cannot be explained simply since one surface would remain on which tunneling could occur, unless the Ar atom disturbs the symmetry sufficiently.

These considerations suggest another model, which includes some aspects of the two-site model and the tunneling model (model III). In this model two localized He atoms are on opposite sites where they occupy diagonally opposite sites at any one time and hop between these two sites possibly in unison. Evidence in favor of such a model comes from recent experiments involving various H₂ isotopomers⁷⁸ and the observation of split lines in other planar molecules of lower symmetry.³⁶ Presently, dedicated path integral Monte Carlo calculations are being carried out to explore the size of the splitting for a more realistic model.⁷⁷

V. Conclusions

The vibronic spectrum of single tetracene molecules embedded in large superfluid ⁴He droplets exhibits a splitting of the 0₀⁰ zero phonon line into two unequal but sharp ($\delta\nu \approx 0.2$ cm⁻¹) peaks separated by about 1 cm⁻¹. The same splitting is observed for the 1a_g vibronic line but disappears when Ar atoms are added to the droplet to form the tetracene-Ar complex and, moreover, is not found with pentacene. Lifetime and hole-burning experiments for the separated lines indicate that both the ground and excited electronic states of tetracene in helium have split levels. The splitting is shown to be compatible with three different simple models involving one or two He atoms of the surrounding superfluid helium that are localized at the surface of the molecule. In one model one atom hops between identical adjacent sites on one face of the molecule. Another model assumes the occupation of two slightly different sites on both sides of the molecules by two localized atoms. The third model postulates a concerted hopping of two atoms, one on the top surface and the other on the bottom surface of the molecule.

The localization of a few helium atoms on the surface of the planar tetracene molecule complements models introduced previously to explain the increased moments of inertia of SF₆ and OCS molecules in He droplets.^{3,5,7} There the effect can be explained by postulating that 8 or 6 He atoms, respectively, are effectively attached to the surface of the molecules and participate in the rotations of the molecules. These numbers are explained in terms of the symmetry of the molecules, and the effect found here is also strongly related to the symmetry.

Additional experiments are being planned to investigate the effect of adding H₂ molecules and its isotopomers to the tetracene molecules.⁷⁸ In these experiments a laser with greater spectral resolution is used.⁷⁹ Path integral Monte Carlo calculations are also being carried out to gain more detailed insight into these new phenomena. Preliminary calculations for benzene indicate a localization of He atoms in the center of this ring molecule.⁸⁰

Very recently, the pulsed seeded beam technique has been improved to such an extent that the ambient temperatures are so low that larger van der Waals clusters of anthracene with up to six attached He atoms can be produced.⁶⁴ It would be intriguing to extend these studies to tetracene to determine the number of He atoms necessary to observe the line splitting reported and analyzed in the present article.

Acknowledgment. We are grateful to Joshua Jortner and Yuri Kagan for several valuable discussions and correspondence. We thank Frank Mielke for his help on the early stages of these experiments and Marius Lewerenz for providing the program with which the calculations in Figure 10 were performed. A.V. and M.H. thank the Deutsche Forschungsgemeinschaft for financial support.

References and Notes

- Toennies, J. P.; Vilesov, A. F. *Annu. Rev. Phys. Chem.* **1998**, *49*, 1.
- Whaley, K. B. *Adv. Molecular Vibrations and Collisional Dynamics*; JAI Press Inc.: Greenwich, CT, 1998; Vol. 3, pp 397–451.
- Hartmann, M.; Miller, R.; Toennies, J. P.; Vilesov, A. F. *Phys. Rev. Lett.* **1995**, *75*, 1566. See also: Fröchtenicht, R.; Toennies, J. P.; Vilesov, A. F. *Chem. Phys. Lett.* **1994**, *229*, 1.
- Harms, J.; Hartmann, M.; Toennies, J. P.; Vilesov, A. F.; Sartakov, B. *J. Mol. Spectrosc.* **1997**, *185*, 204.
- Hartmann, M.; Pörtner, N.; Sartakov, B.; Toennies, J. P.; Vilesov, A. F. *J. Chem. Phys.* **1999**, *110*, 5109.
- Grebenev, S.; Toennies, J. P.; Vilesov, A. F. *Science* **1998**, *279*, 2083.
- Grebenev, S.; Hartmann, M.; Havenith, M.; Sartakov, B.; Toennies, J. P.; Vilesov, A. F. *J. Chem. Phys.* **2000**, *112*, 4485.
- Fröchtenicht, R.; Kaloudis, M.; Koch, M.; Huisken, F. *J. Chem. Phys.* **1996**, *105*, 6128.
- Blume, D.; Lewerenz, M.; Huisken, F.; Kaloudis, M. *J. Chem. Phys.* **1996**, *105*, 8666.
- Behrens, M.; Buck, U.; Fröchtenicht, R.; Hartmann, M.; Huisken, F.; Rohmund, F. *J. Chem. Phys.* **1994**, *109*, 5914.
- Callegari, C.; Conjusteau, A.; Reinhardt, I.; Lehmann, K. K.; Scoles, G.; Dalfovo, F. *Phys. Rev. Lett.* **1999**, *83*, 5058.
- Harms, J.; Hartmann, M.; Sartakov, B.; Toennies, J. P.; Vilesov, A. F. *J. Chem. Phys.* **1999**, *110*, 5124.
- Sindzingre, B. P.; Klein, M. L.; Ceperley, D. M. *Phys. Rev. Lett.* **1989**, *63*, 1601.
- Hartmann, M.; Mielke, F.; Toennies, J. P.; Vilesov, A. F.; Benedek, G. *Phys. Rev. Lett.* **1996**, *76*, 4560.
- Barnett, R. N.; Whaley, K. B. *J. Chem. Phys.* **1993**, *99*, 9730.
- Dalfovo, F. *Z. Phys. D* **1994**, *29*, 61.
- Stinkemeier, F.; Ernst, W. E.; Higgins, J.; Scoles, G. *J. Chem. Phys.* **1995**, *102*, 615.
- Higgins, J.; Callegari, C.; Reho, J.; Stinkemeier, F.; Ernst, W. E.; Lehmann, K.; Gutowski, M.; Scoles, G. *Science* **1996**, *273*, 629.
- Rebane, K. K. *Chem. Phys.* **1994**, *189*, 139. Rebane, K. K. *Impurity Spectra of Solids*; Plenum Press: New York, 1970.
- Tilley, D. R.; Tilley, J. *Superfluidity and Superconductivity*, 3rd ed.; Adam Hilger: Bristol, 1996; pp 31–71.
- Glyde, H. R. *Excitations in Liquid and Solid Helium*; Oxford University Press: New York, 1995.
- Persistent Spectral Hole-Burning: Science and Applications*; Moerner, W. E., Ed.; Topics in Current Physics 44; Springer: Berlin, 1988.
- Single-Molecule Optical Detection, Imaging and Spectroscopy*; Basché, T.; Moerner, W. E.; Orrit, M.; Wild, U. P., Eds.; VCH Verl. D69451: Weinheim, 1997.
- Amirav, A.; Even, U.; Jortner, J. *J. Chem. Phys.* **1981**, *75*, 3770.
- Amirav, A.; Even, U.; Jortner, J. *Chem. Phys. Lett.* **1980**, *72*, 21.
- Amirav, A.; Even, U.; Jortner, J. *J. Phys. Chem.* **1981**, *85*, 309.
- Leutwyler, S.; Jortner, J. *J. Phys. Chem.* **1987**, *91*, 5558.
- van Herpen, W. M.; Merts, W. L.; Dymanus, A. *J. Chem. Phys.* **1987**, *87*, 182.
- Ben-Horin, N.; Even, U.; Jortner, J.; Leutwyler, S. *J. Chem. Phys.* **1992**, *97*, 5296.
- Dick, B.; Zinghar, E.; Haas, Y. *Chem. Phys. Lett.* **1991**, *187*, 571.
- Kaervell, A.; Wilkinson, F. *Chem. Phys. Lett.* **1971**, *11*, 472.
- Lindinger, A.; Toennies, J. P.; Vilesov, A. F. *J. Chem. Phys.* **1999**, *110*, 1429.
- Close, J. D.; Federmann, F.; Hoffmann, K.; Quaaas, N. *Chem. Phys. Lett.* **1997**, *276*, 393.
- Lugovoj, E.; Toennies, J. P.; Vilesov, A. F. *J. Chem. Phys.*, **2000**, *112*, 8217.
- Lindinger, A. Dissertation, University of Göttingen, Max-Planck-Institut für Strömungsforschung, Bericht 18/1997.
- Lindinger, A.; Lugovoj, E.; Toennies, J. P.; Vilesov, A. F. *Z. Phys. Chem.* **2001**, *3*, 401.
- Hartmann, M.; Lindinger, A.; Toennies, J. P.; Vilesov, A. F. Manuscript in preparation.
- Hartmann, M.; Lindinger, A.; Toennies, J. P.; Vilesov, A. F. *Chem. Phys.* **1998**, *239*, 139.
- Hartmann, M. Dissertation, externer Bericht 10/1997, Max-Planck-Institut für Strömungsforschung, 1997.
- Lee, E.; Farrelly, D.; Whaley, K. B. *Phys. Rev. Lett.* **1999**, *83*, 3812.
- Buchenau, H.; Knuth, E. L.; Northby, J.; Toennies, J. P.; Winkler, C. *J. Chem. Phys.* **1990**, *92*, 6875.
- Lewerenz, M.; Schilling, B.; Toennies, J. P. *Chem. Phys. Lett.* **1993**, *206*, 381.
- Junk, G.; Svec, H. *J. Am. Chem. Soc.* **1963**, *85*, 839.

- (44) Gaffney, J. S.; Pierce, R. C.; Friedmann, L. *J. Am. Chem. Soc.* **1977**, *99*, 4293. Lias, S. G.; Bartmess, J. E.; Liebman, J. F.; Holmes, J. L.; Levin, R. P.; Mallard, W. G. *J. Phys. Chem. Ref. Data* **1988**, *17*, Suppl. 1, 861.
- (45) Aldrich Chemical Co.
- (46) The actual effective tetracene pressures in the scattering cell were calculated from the pressure corresponding to the maximum in the Poisson curve for capture of a single molecule. This is given by $P_{\max}(n=1) = k_B T (\sigma I F_{a_0})^{-1}$ where k_B is Boltzmann's constant, σ is the capture cross section, and F_{a_0} is a factor that accounts for the dependence of the number of collisions on the finite velocity of the primary beam. By assuming a capture cross section equal to the area of the droplet ($\sigma = 15.5 \text{ N}^{2/3} \text{ \AA}^2$) $P_{\max}(n=1)$ is estimated to be 0.8×10^{-4} mbar.
- (47) Lewerenz, M.; Schilling, B.; Toennies, J. P. *J. Chem. Phys.* **1995**, *102*, 8191.
- (48) Lambda Physik model, LPD 3000.
- (49) Hamamatsu model RS 943-02.
- (50) Stanford Research model SR-255.
- (51) Fast Com Tec Daten-system Model 7885, 82041 Oberhaching, Germany.
- (52) Jortner, J.; Ben-Horin, N. *J. Chem. Phys.*, **1993**, *98*, 9346. Jortner, J. *J. Chim. Phys.* **1995**, *92*, 205.
- (53) Lindinger, A.; Toennies, J. P.; Vilesov, A. F. *Phys. Chem. Chem. Phys.*, in print.
- (54) Knuth, E. L.; Schaper, S.; Toennies, J. P. *Atomic and Molecular Beams*; Camparque, R., Ed.; Springer: Berlin, 2001; pp 839–846.
- (55) Heinecke, E.; Hartmann, D.; Müller, R.; Hese, A. *J. Chem. Phys.* **1998**, *109*, 906.
- (56) Unpublished.
- (57) Gordon, E. B.; Shestakov, A. F. *Low Temp. Phys.* **2000**, *26*, 1.
- (58) Kwon, Y.; Whaley, K. B. *Phys. Rev. Lett.* **1999**, *83*, 4108.
- (59) Kwon, Y.; Huang, P.; Patel, M.; Blume, D.; Whaley, K. B. *J. Chem. Phys.* **2000**, *113*, 6469.
- (60) Lauter, H. J.; Godfrin, H.; Leiderer, P. *J. Low. Temp. Phys.* **1992**, *87*, 425.
- (61) Treiner, J. *J. Low Temp. Phys.* **1993**, *92*, 1.
- (62) Beck, S. M.; Liverman, M. G.; Monts, D. L.; Smalley, R. E. *J. Chem. Phys.*, **1979**, *70*, 232.
- (63) Bernstein, E. R.; Law, K.; Schauer, M. *J. Chem. Phys.* **1984**, *80*, 634.
- (64) Even, U.; Jortner, J.; Noy, D.; Cossart-Magos, C. *J. Chem. Phys.* **2000**, *112*, 8068.
- (65) Smalley, R. E.; Wahrton, L.; Levy, D. H.; Chandler, D. W. *J. Chem. Phys.*, **1978**, *68*, 2487.
- (66) Hager, H.; Wallace, S. C. *J. Phys. Chem.* **1983**, *87*, 2121.
- (67) DeHaan, D. O.; Holton, A. L.; Zwiier, T. S. *J. Chem. Phys.* **1989**, *90*, 3952.
- (68) The maximum in the pair correlation function at $T = 1.0$ K measured by neutron scattering is at 3.47 \AA [Svensson, E. C.; Sears, V. F.; Woods, A. B. D.; Mortel, P. *Phys. Rev. B* **1980**, *21*, 3638.
- (69) Even, U.; Amirav, A.; Leutwyler, S.; Ondrechen, M. J.; Berkovitch-Yellin, Z.; Jortner, J. *Faraday Discuss. Chem. Soc.* **1982**, *73*, 153.
- (70) Yamanouchi, K.; Isogai, S.; Tsuchiya, S.; Kuchitsu, K. *Chem. Phys.* **1987**, *116*, 123.
- (71) The computer code used for these calculations was written bei Marius Lewerenz.
- (72) McMahan, A. K. *J. Low Temp. Phys.* **1972**, *8*, 159.
- (73) Glyde, H. R.; Svensson, E. C. *Methods Exp. Phys.* **1987**, *23B*, 303, p 311.
- (74) Guyer, R. A.; Richardson, R. C.; Zane, L. I. *Rev. Mod. Phys.* **1971**, *43*, 532.
- (75) Ceperley, D. M. *Rev. Mod. Phys.* **1996**, *67*, 279.
- (76) Zilm, K. W.; Millar, J. M. *Adv. Magn. Opt. Reson.* **1990**, *15*, 163.
- (77) Huang, P.; Whaley, B. Private communication, 1998.
- (78) Pörtner, N.; Toennies, J. P.; Vilesov, A. F. Manuscript in preparation.
- (79) Lindinger, A.; Stienkemeier, F.; Pörtner, N.; Toennies, J. P.; Vilesov, A. F. Unpublished.
- (80) Kwon, Y.; Whaley, K. B. *J. Chem. Phys.* **2001**, *114*, 3163.